THE JOURNAL OF PHYSICAL CHEMISTRY C
A JOURNAL OF THE AMERICAN CHEMICAL SOCIETY

pubs.acs.org/JPCC

Article

Theoretical Understanding of Dynamic Catalysis

Pankaj Jangid, Srabanti Chaudhury,[#,*] and Anatoly Kolomeisky[#,*]

Cite This: *J. Phys. Chem. C* 2024, 128, 9077−9089

Read Online

ACCESS | Metrics & More | Article Recommendations | Supporting Information

ABSTRACT: Dynamic catalysis is a phenomenon in which the catalytic properties of the system change with time. It has been recently proposed as an alternative to the current widely utilized static catalytic approach because of potential significant improvements in catalytic efficiency. Dynamic restructuring of active sites on surfaces has also been observed in some nanocatalysts. However, the microscopic mechanisms of underlying processes remain not well understood. We developed a new stochastic framework that allows us to quantitatively describe dynamic catalysis and compare its properties with the static approach. It is found that fluctuations between different catalytic pathways might lead to enhancements in chemical reaction rates but only for specific ranges of kinetic parameters. Our theoretical method can explain these observations from the microscopic point of view. We show that the temporal efficiency of dynamic catalysis depends only on the rates of chemical reactions and transitions between different catalytic pathways while being independent of the number of active sites. It is also argued that the effects of dynamic catalysis are purely nonequilibrium, and the associated energy dissipation is the source of improvements in catalytic efficiency. In addition, the stochasticity of dynamic catalysis is investigated. The proposed theoretical approach clarifies some important microscopic aspects of catalytic processes.

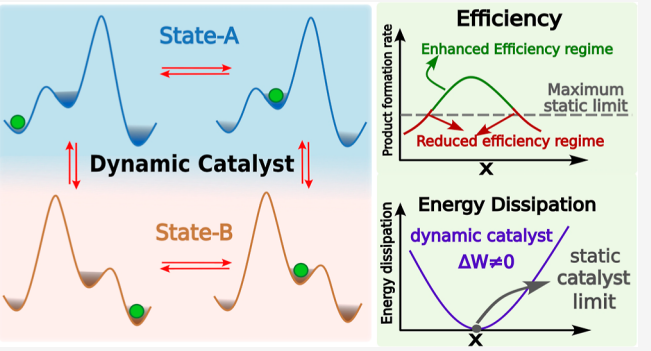

INTRODUCTION

Catalysis is a method of accelerating chemical reactions that is widely utilized in various industrial processes for manufacturing consumer goods, fuels, fertilizers, plastics, medicines, polymers, and many other things. It is also critically important for multiple applications in modern chemical research.[1−4] For many years, significant research efforts have been devoted to the search for the materials with the most efficient and selective properties that led to the emergence of several new classes of catalysts such as metal−organic frameworks,[5,6] zeolites,[7] nanoparticles,[8] and many others. Catalysis has also been investigated by a wide spectrum of theoretical methods ranging from advanced quantum mechanical calculations to computer simulations and machine-learning techniques.[9−14] However, many aspects of microscopic mechanisms of catalytic processes still remain not well understood.

Essentially, all currently utilized catalytic methods can be viewed as *static catalysis* since the properties of the active sites in these systems typically do not change with time (or are assumed to be constant). Significant efforts have been devoted to developing catalytic systems in which the binding characteristics of surface-associated substrate species and transition states can be tuned to achieve the maximum catalytic turnover frequency.[15] However, there is a fundamental result, which is known as the Sabatier principle, that limits further improvements of catalytic systems.[16,17] It states that the most optimal conditions for catalysis can be achieved when the interactions between catalysts and the substrate molecules are of intermediate strength. For too weak interactions, the substrates do not want to associate with active sites, lowering the overall rate of the process. For too strong interactions, the product formation is significantly delayed, again lowering the overall chemical rate. This leads to so-called volcano-type relationships between catalytic rates and the strength of substrate−catalyst molecular bonds, and the peak in such curves corresponds to the upper limit of catalytic performance.[17,18] This also means, however, that it is impossible to improve the catalytic properties of the system beyond this optimal set of conditions.

A new approach that might overcome the fundamental limitations of the Sabatier principle has been proposed recently.[19,20] The main idea here is to deviate from the static catalysis conditions and consider situations when catalytic properties can fluctuate with time. This new approach can be viewed as *dynamic catalysis*. Unlike static catalysts, the performance of which is limited by the Sabatier principle, in dynamic catalysts, if the system is trapped in one surface state

Received: April 25, 2024
Revised: May 14, 2024
Accepted: May 15, 2024
Published: May 23, 2024

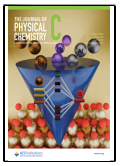

https://doi.org/10.1021/acs.jpcc.4c02713
J. Phys. Chem. C 2024, 128, 9077−9089

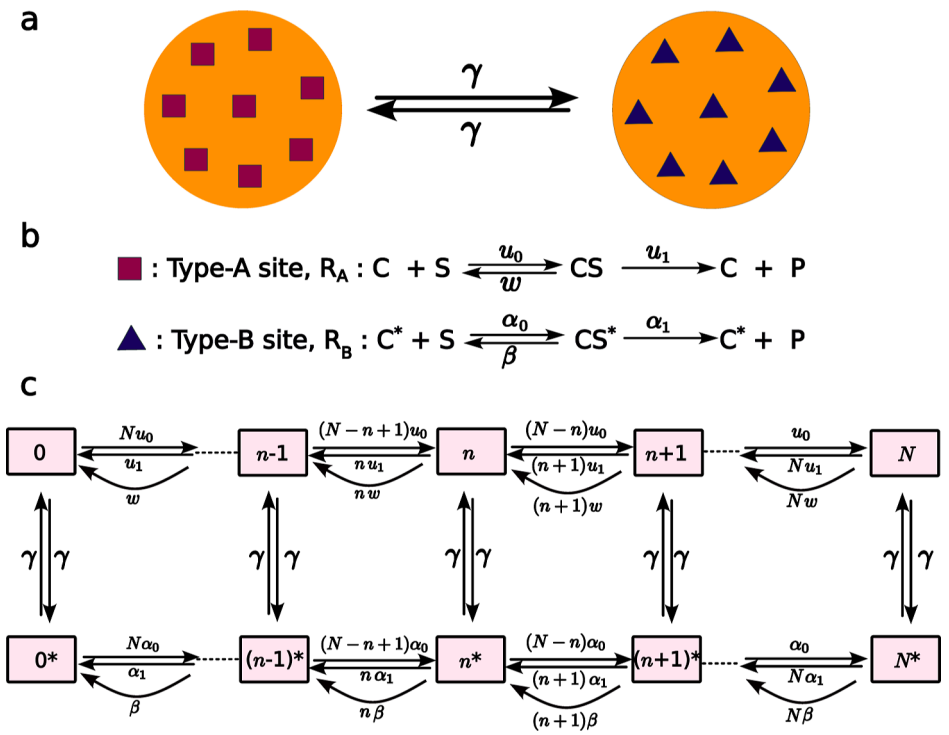

Figure 1. Discrete-state stochastic model of dynamic catalysis. (a) Schematic representation of a single catalytic particle that can transition between two surface states with catalytically different active sites. (b) Molecular mechanisms of chemical reactions catalyzed on the active sites of type A (squares) and type B (triangles). (c) Effective chemical-kinetic description for processes taking place in dynamic catalysis.

due to a large barrier on the path to the product, the dynamic transition to another state might help to escape the trap.[21] It has been suggested that such modifications of the catalytic surfaces might lead to higher catalytic efficiency and faster overall reaction rates.[19,20] The catalytic surfaces can be altered by applying external electric fields and mechanical forces or subjecting them to light or electromagnetic waves to induce charge fluctuations.[22] It is also possible to alternate the chemical medium of the system (pH, ionic strength, etc.) to achieve dynamic catalysis conditions. Some initial experimental observations are supporting the idea that catalytic efficiency can be improved in dynamic catalysis.[22] However, it is still unclear under what conditions such improvements can be made and what is the degree of catalytic enhancement. It is also unknown why it might happen at the more microscopic level.

Closely related to dynamic catalysis are stochastic pumping phenomena where the relative stabilities of states within a cycle are modified by employing a time-dependent external energy source or nonequilibrium chemical reactions. This modulation influences the rate constants for transitions between states in a correlated manner, leading to a net flux through the cycle and enabling work in the system. Resonant catalysts, based on stochastic pumping, employ a time-dependent oscillatory external perturbation that deterministically alters the energies of reaction species.[19−22] Within a specific range of oscillation frequency, known as the resonating frequency, the catalyst's turnover time experiences significant enhancement, as observed in the work by Dauenhauer and colleagues in catalysis applications.[19−22] More recently, stochastic pumping principles have been applied to investigate catalytic molecular machines, where periodic changes in the catalytic environment, induced by time-varying temperature, are explored.[23]

In close resemblance to dynamic catalysis is the phenomenon of *fluxionality* of catalytic active sites that has been found in several systems.[24−26] In this case, the active sites can quickly interconvert between multiple thermally accessible states, but each of them might have different catalytic properties. Recent progress in experimental techniques has unveiled the dynamic nature of nanoparticle catalyst surfaces under reaction conditions. Notably, Pd and Pt nanoparticle surfaces exhibit oscillatory behavior during the CO oxidation reaction.[27,28] This dynamic response challenges the traditional notion of static catalyst surfaces and is linked to factors such as surface coverage and elevated temperatures of the nanoparticles. The observed oscillatory behavior provides valuable insights into the complex dynamics of catalytic processes at the nanoscale.[27−30] There are several catalytic systems where fluxionality has been experimentally investigated. For example, it has been confirmed for some chemical reactions on CeO_2 and CeO_2-supported Pt nanoparticles.[28,31] It has been studied also by various spectroscopic and electron microscopy methods.[32] Interestingly, some metal nanoclusters demonstrated dynamic meta-stability at the atomic scale. These catalytic clusters exhibited multiple low-energy isomeric states, representing distinct structural configurations of identical sets of atoms.[14,33−36] So far, the dynamic restructuring of catalytic active sites has been observed on several bulk catalytic surfaces, in some nanoparticle systems, and also in the supported nanocluster catalysts.[14,33−36] However, the underlying microscopic picture of catalytic processes in these systems also remains not fully understood.

The observations of time-dependent changes in the catalytic properties of active sites have raised several important fundamental questions. Is dynamic catalysis always more efficient than static catalysis? However, if yes, what is the microscopic reason for this? If not, for what ranges of kinetic

https://doi.org/10.1021/acs.jpcc.4c02713
J. Phys. Chem. C 2024, 128, 9077−9089

parameters can it be achieved and why? What is the driving force behind the possible enhancements of catalytic performance in dynamic catalysis? In this work, we present a theoretical investigation that attempts to answer these questions quantitatively. Our goal is to obtain a more microscopic picture of underlying processes by concentrating on studying dynamic properties of these catalytic systems. More specifically, we developed a minimal theoretical model to investigate the catalytic properties of dynamic catalysis and to compare them with static catalysis. The idea is to use the simplest theoretical model that can clarify the physics of these complex phenomena. Our analysis, which is based on discrete-state stochastic calculations, suggests that the increase in catalytic efficiency can be achieved but only for some specific ranges of kinetic parameters. Our theory provides physical–chemical arguments to explain these observations. In addition, it is found that dynamic catalysis is always operating under nonequilibrium conditions, and the associated energy dissipation is the main source of the catalytic enhancements in comparison with static catalysis. Furthermore, the stochasticity of catalytic turnover times in dynamic catalysis exhibits a complex behavior that can be explained by our theoretical approach.

METHODS

To understand the molecular mechanisms of dynamic catalysis, let us start with the model schematically shown in Figure 1a. This model is motivated by several studies, where a single nanocluster catalyst can have multiple isomeric structures with different catalytic activities, and there are stochastic thermally driven transitions between these states[14,33−36] However, for a clear comparative analysis, only two types of different catalytic surfaces, labeled as A and B, are assumed in the system. We consider a single catalytic particle with N identical active sites, where the surface can be found in one of two macrostates: with all active sites being of type A (squares) or with all active sites being of type B (triangles). It is assumed for simplicity that the chemical reaction of transformation of substrate S into product P is catalyzed via two different Michaelis–Menten-like mechanisms on the sites A and B (with the same final product), respectively, as shown in Figure 1b. On A sites, the substrate can associate to the active site with a rate u_0, while the reverse rate is equal to w. Then, the product can be created with a rate u_1 from the substrate–catalyst complex CS. Similarly, on B sites, the substrate can associate with the active site with a rate α_0, while the reverse rate is equal to β, and the product can be created with a rate α_1 from the substrate–catalyst complex CS*. The system fluctuates between two surface macrostates with a rate γ. To assist the readers, all parameters utilized in our analysis are assembled and explained in Table 1.

At any moment, every active site can be found in one of the four microstates: free A site, free B site, occupied by the CS complex for A site, and occupied by the CS* complex for B site. Then, one can introduce an effective chemical-kinetic scheme to describe the processes in the system, as presented in Figure 1c. In this scheme, the state n corresponds to the situation when the system is in the macrostate A with n active sites occupied by the complexes CS. The state n^* describes the situation when the system is in the macrostate B with n active sites occupied by the complexes CS*. From any effective state n or n^*, the system can transition to the state $(n-1)$ or $(n-1)^*$, respectively, by forming a product P or by the dissociation of the complex CS/CS* back into the substrate and the free site. The corresponding transition rates are given by $n(u_1+w)$ and $n(\alpha_1+\beta)$, respectively; see Figure 1c. The factor n here is because there are n such complexes from which these processes might occur. The system can also transition to the states $(n+1)$ and $(n+1)^*$, respectively, and this happens only via the association of the substrate to the free active sites. The corresponding rates are $(N-n)u_0$ and $(N-n)\alpha_0$; see Figure 1c. The factor $(N-n)$ corresponds to the number of available active sites not covered by the substrate/catalyst complexes. Furthermore, the system can reversibly fluctuate between the states n and n^* with the rate γ (Figure 1c), reflecting the dynamic nature of the system. It is important to note that mapping catalytic processes in the system into effective kinetic

Table 1. All Parameters and Their Explanations Utilized in Our Theoretical Method

symbol	description
C	catalytic site of type-A
C*	catalytic site of type-B
S	substrate molecule
CS	substrate–catalyst complex on type-A site
CS*	substrate–catalyst complex on type-B site
P	product molecule
N	total active sites on the catalyst
N	effective state with n sites in CS state
n^*	effective state with n sites in CS* state
u_0	rate of binding of S on C
u_1	rate of forming a product from the CS complex
w	rate of dissociation of CS into C and S
α_0	rate of binding of S on C*
α_1	rate of forming a product from the CS complex
β	rate of dissociation of CS into C and S
γ	rate of transition from type-A to type-B and type-B to type-A
$F_n(t)$	probability density function of product formation at time t starting from state n and n at $t=0$
$F_{n^*}(t)$	probability density function of product formation at time t starting from state n^* at $t=0$
$\tilde{F}_n(s)$ $\tilde{F}_{n^*}(s)$	Laplace transform of $F_n(t)$ and $F_{n^*}(t)$, respectively
$\langle T_n\rangle$, $\langle T_{n^*}\rangle$	mean first passage time of product formation from state n and n^*, respectively
$\langle T_n^2\rangle$, $\langle T_{n*}^2\rangle$	Mean-squared first passage time of product formation from state n and n^*, respectively
f_n, f_{n^*}	weight factors (probability of product formation from state n and n^*, respectively)
P_n, P_{n^*}	steady-state probability of finding the system in state n and n^*, respectively
$\langle\tau\rangle$	mean product formation time from the whole catalyst
$\langle\tau^2\rangle$	Mean-squared product formation time from the whole catalyst
EF	efficiency function, the ratio of product formation time of the static and dynamic catalyst
X	a dimensionless parameter giving the relation between type-A and type-B catalytic activities
γ_{c1}, γ_{c2}, x	critical values of γ and x
P_n	steady-state probability distribution of state n
J_{ij}	net steady-state flux from state i to state j
r_{ij}	transition rate for state i to state j transition
A_{ij}	affinity of transition from state i to j
ΔW	energy dissipation (entropy production) rate
η	energy efficiency parameter
R	randomness parameter

https://doi.org/10.1021/acs.jpcc.4c02713
J. Phys. Chem. C 2024, 128, 9077−9089

scheme in Figure 1c allows us to simultaneously account for chemical reactions taking place at all active sites.

Although the analysis can be done for an arbitrary number of active sites N and an arbitrary number of intermediate states (see the case of the systems with more than one intermediate state presented in the Supporting Information), to simplify calculations and to understand better the microscopic picture of dynamic catalysis, it is convenient to consider the simplest nontrivial catalytic system where the surface has only two active sites ($N = 2$) with one intermediate state in each pathway. Theoretical analysis can be easily generalized for an arbitrary number of active sites. To obtain the dynamic properties of the $N = 2$ system, we utilize a method of first-passage probabilities that has already been successfully utilized for studying the dynamics of catalyzed reactions.[12,13,37,38]

At any instant of time, the catalyst can be found in the effective state n (the system follows the pathway A) or in the state n^* (the system follows the pathway B). Now, one can define a function $F_n(t)$ as a probability density function of the first product formation event to be observed at time t after starting initially ($t = 0$) from the state n (when the catalyst is in the macrostate A with n occupied active sites ready to make a product molecule). Similarly, $F_{n^*}(t)$ is the probability density function of observing the first product formation at time t starting initially in the state n^* (when the catalyst is in the macrostate B with n occupied sites ready to make a product molecule). Note that the first-passage events that we record correspond to transitions from the state n (n^*) to the state $n - 1$ ($n^* - 1$) that take place with the rates nu_1 ($n\alpha_1$); see Figure 1c. We also record separately transitions $n \to n - 1$ ($n^* \to n^* - 1$) that occur with the rates nw ($n\beta$) due to dissociations of the intermediate substrate-active site complex. The time evolution of these first-passage probability functions is governed by the backward master equations

$$\begin{aligned}
\frac{dF_0(t)}{dt} &= 2u_0F_1(t) + \gamma F_{0^*}(t) - (2u_0 + \gamma)F_0(t);\\
\frac{dF_{0^*}(t)}{dt} &= 2\alpha_0F_{1^*}(t) + \gamma F_0(t) - (2\alpha_0 + \gamma)F_{0^*}(t);\\
\frac{F_1(t)}{dt} &= u_1F_p(t) + wF_0(t) + u_0F_2(t) + \gamma F_1^*(t)\\
&\quad - (u_0 + u_1 + w + \gamma)F_1(t);\\
\frac{F_{1^*}(t)}{dt} &= \alpha_1F_p(t) + \beta F_{0^*}(t) + \alpha_0F_{2^*}(t) + \gamma F_1(t)\\
&\quad - (\alpha_0 + \alpha_1 + \beta + \gamma)F_{1^*}(t);\\
\frac{dF_2(t)}{dt} &= 2u_1F_p(t) + 2wF_1(t) + \gamma F_{2^*}(t)\\
&\quad - [2(u_1 + w) + \gamma]F_2(t);\\
\frac{dF_{2^*}(t)}{dt} &= 2\alpha_1F_p(t) + 2\beta F_{1^*}(t) + \gamma F_2(t)\\
&\quad - [2(\alpha_1 + \beta) + \gamma]F_{2^*}(t).
\end{aligned} \tag{1}$$

Here, $F_p(t) = \delta(t)$ is the initial condition, indicating that starting from a product state leads to immediate product formation. The above set of algebraic equations can be solved using Laplace transformations, where $\mathcal{L}\{F_n(t)\} = \tilde{F}_n(s) = \int_0^\infty e^{-st}F_n(t)\,dt$ and $\mathcal{L}\{F_{n^*}(t)\} = \tilde{F}_{n^*}(s) = \int_0^\infty e^{-st}F_{n^*}(t)\,dt$. The details of calculations are presented in the Supporting Information.

To obtain the dynamic properties of dynamic catalysis on the surfaces alternating between two types of active sites, we introduce $\langle T_n\rangle$, $\langle T_{n^*}\rangle$, and $\langle T_n^2\rangle$, $\langle T_{n*}^2\rangle$ as the mean first-passage time and mean-squared time, respectively, of product formation from the state n or n^*. These quantities are directly obtained from the first-passage probability functions

$$\langle T_n\rangle = -\left.\frac{d\tilde{F}_n(s)}{ds}\right|_{s=0}, \qquad \langle T_n^2\rangle = \left.\frac{d^2\tilde{F}_n(s)}{ds^2}\right|_{s=0} \tag{2}$$

and

$$\langle T_{n^*}\rangle = -\left.\frac{d\tilde{F}_{n^*}(s)}{ds}\right|_{s=0}, \qquad \langle T_{n*}^2\rangle = \left.\frac{d^2\tilde{F}_{n^*}(s)}{ds^2}\right|_{s=0} \tag{3}$$

Now, the mean reaction time to form the product from any state of the system can be evaluated as a weighted sum of mean first-passage times from all possible initial states

$$\langle\tau\rangle = f_0\langle T_0\rangle + f_{0^*}\langle T_{0^*}\rangle + f_1\langle T_1\rangle + f_{1^*}\langle T_{1^*}\rangle \tag{4}$$

where the weighting factors f_n or f_{n^*} can be estimated using the following arguments.[37] We are assuming that the system is already in the stationary state, and then to start from the given state n or n^*, the product formation should drive the system to this state. In other words, these probabilities must be proportional to the fluxes leading to these states. For example, since no new reaction can start from states 2 and 2* (all sites are occupied), their contribution to the mean reaction time is zero. However, the contributions from the states 0, 0*, 1, and 1* are possible because the reaction can start from the available free sites.

In the steady state, the flux to start a reaction from the state n (n^*) equals the flux to end a reaction (via the product formation) at the same state n (n^*). Therefore, we can write ($n = 0, 1$)

$$f_n \propto (n + 1)u_1P_{n+1}, \qquad f_{n^*} \propto (n + 1)\alpha_1P_{(n+1)^*} \tag{5}$$

where P_n and P_{n^*} are steady-state probabilities to find the system in the state n or n^*, respectively. These stationary probabilities can be explicitly evaluated, as shown in the Supporting Information. Since f_n and f_{n^*} are probabilities that must be normalized, it yields

$$\begin{aligned}
f_n &= \frac{(n + 1)u_1P_{n+1}}{\sum_{n=0}^{1}(n + 1)(u_1P_{n+1} + \alpha_1P_{(n+1)^*})},\\
f_{n^*} &= \frac{(n + 1)\alpha_1P_{(n+1)^*}}{\sum_{n=0}^{1}(n + 1)(u_1P_{n+1} + \alpha_1P_{(n+1)^*})}
\end{aligned} \tag{6}$$

Using eqs 4 and 6 and the results for the stationary probabilities (see the Supporting Information), the mean reaction times can be explicitly evaluated as

$$\langle\tau\rangle = \frac{(u_0 + u_1 + w)(\alpha_0 + \alpha_1 + \beta) + (u_0 + u_1 + w + \alpha_0 + \alpha_1 + \beta)\gamma}{\alpha_0\alpha_1(u_0 + u_1 + w) + u_0u_1(\alpha_0 + \alpha_1 + \beta) + (u_0 + \alpha_0)(u_1 + \alpha_1)\gamma} \tag{7}$$

Our analysis can be easily generalized for more general situations with unequal stochastic fluctuation rates between different catalytic pathways, as shown in the Supporting

https://doi.org/10.1021/acs.jpcc.4c02713
J. Phys. Chem. C 2024, 128, 9077−9089

Information. In the limit of very fast fluctuations ($\gamma \gg 1$), the expression simplifies into

$$\langle \tau \rangle = \frac{(u_0 + u_1 + w + \alpha_0 + \alpha_1 + \beta)}{(u_0 + \alpha_0)(u_1 + \alpha_1)} \tag{8}$$

This limiting case can be easily explained using our theoretical approach (see also Figure 1c). In this case, the local equilibrium between states A and B is achieved, and the overall process can be viewed as a catalytic process on only one "average" type of active sites with the effective complex formation rates $(u_0 + \alpha_0)/2$, the effective complex dissociation rates $(w + \beta)/2$, and the effective product formation rates $(u_1 + \alpha_1)/2$. The choice of equal γ for both transitions implies that the likelihood of encountering A and B macrostates will be equal over an extended observation period of the catalyst. On the other hand, different fluctuation rates suggest that the catalytic surface prefers a specific macrostate, where the catalyst tends to stay for longer duration, on average. As shown in the Supporting Information (Figure S7), the qualitative analysis of our catalytic properties of dynamic catalysis remains consistent for different transition rates between A and B macrostates.

The higher moments of the reaction times can also be calculated following the same procedure. For example, the mean-squared reaction times are given by

$$\langle \tau^2 \rangle = f_0 \langle T_0^2 \rangle + f_{0^*} \langle T_{0*}^2 \rangle + f_1 \langle T_1^2 \rangle + f_{1^*} \langle T_{1*}^2 \rangle \tag{9}$$

The mean-squared first-passage times can be obtained from the first-passage probabilities, as specified in eqs 2 and 3.

RESULTS AND DISCUSSION

To obtain properties of dynamic catalysis, let us define a parameter x that connects the transition rates in different catalytic states of the system

$$\alpha_0 = u_0 x \qquad \alpha_1 = \frac{u_1}{x} \tag{10}$$

The physical meaning of this parameter is the following. It gives the ratio of how fast the first transition rate of substrate binding to the active site when the surface has only B sites in comparison with the same transition when the surface has only A sites. Simultaneously, it gives the ratio of how fast the second transition rate of product formation is when the surface has only A sites in comparison with the product formation rate when the surface has only B sites. Introducing a single parameter x reduces the parameter space and makes the analysis easier. It is important to note that eq 10 describes the simplest situation, and more complex relations between the transition rates in different pathways are possible. However, as we show explicitly in the Supporting Information, results do not change much for more general cases. Thus, to better clarify the physics of dynamic catalysis, we concentrate on this simplest case that can be viewed as the situation when the transition states in both pathways are close to each other along the reaction coordinate of product formation (see the Supporting Information).

Furthermore, relating the rates by the single parameter satisfies the Sabatier principle where the rate of adsorption and desorption cannot be varied independently for a catalyst. If the energy of the CS complex is low, then the rate of forming the CS will be faster. Additionally, the rate of forming the product from CS will be slower because of the larger barrier for this transition. Therefore, two catalytic pathways with low and high adsorption rates will have high and low desorption rates, respectively. In addition, one can think of $k_B T \ln(x)$ as an energy scale that specifies the corresponding differences in energy barriers. When $x = 1$, there are no differences between the two catalytic pathways to make products (via sites A or via sites B). This case effectively corresponds to the limit of static catalysis. For $x > 1$, the substrate association is faster for the catalytic pathway via the states B, and the product formation is faster for the catalytic pathway via the states A. The opposite situation is observed for $x < 1$.

One should also notice that eq 10 is consistent with the Sabatier principle. It postulates that accelerating the substrate-binding reaction step simultaneously leads to slowing the product formation step and vice versa. It also implicitly assumes that the sum of activation barriers for two different catalytic pathways is the same

$$E_{C\to CS} + E_{CS\to P} = E_{C^*\to CS^*} + E_{CS^*\to P} \tag{11}$$

because from eq 10, we have

$$E_{C^*\to CS^*} = E_{C\to CS} - k_B T \ln(x),$$
$$E_{CS^*\to P} = E_{CS\to P} + k_B T \ln(x) \tag{12}$$

One can consider more general kinetic rates that are not bound by the condition given in eq 11, but this should not change the mechanisms of dynamic catalysis. For this reason, we choose to utilize a single parameter x that reduces the parameter space in our system, allowing us to obtain a clearer microscopic picture of underlying processes.

Temporal Efficiency of the Catalyst: Static vs Dynamic. The most popular property to evaluate the catalytic system is its turnover frequency (or mean reaction time). In our theoretical framework, we can explicitly calculate these rates for both static ($\langle \tau \rangle_s$) and dynamic catalysis systems ($\langle \tau \rangle_d$). One can then define a dimensionless temporal efficiency parameter EF, which is the ratio of these reaction times

$$\mathrm{EF} = \frac{\langle \tau \rangle_s}{\langle \tau \rangle_d} \tag{13}$$

It is important to notice here that although our calculations are done for the case of only $N = 2$ active sites, the result for the efficiency parameter is valid for *arbitrary* N. This is because each active site is independent of the other, and the overall reaction times are expected to be proportional to $1/N$, which means that the ratio of these times is independent of N. These arguments emphasize the importance of eq 13 since the efficiency depends only on the individual rates from chemical reactions and fluctuation rates but not on the number of active sites.

When EF > 1, dynamic catalysis is faster, while for EF < 1, static catalysis is a more efficient approach. We can explicitly evaluate the efficiency parameter using eqs 7 and 10, leading to

$$\begin{aligned}\mathrm{EF} = \{&(u_0 + u_1 + w)[(u_1 + \gamma) + (u_0 + u_1 + 2\gamma + 2w)x \\ &+ (u_0 + \gamma)x^2]\}/\{2((u_0 + u_1 + w + \gamma)u_1 \\ &+ [(u_0 + u_1 + w)w + (u_0 + u_1 + 2w)\gamma]x \\ &+ u_0(u_0 + u_1 + w + \gamma)x^2)\}\end{aligned} \tag{14}$$

https://doi.org/10.1021/acs.jpcc.4c02713
J. Phys. Chem. C 2024, 128, 9077−9089

where for simplicity, we also assumed that the backward reaction rates in both catalytic pathways are the same, i.e., $\beta = w$. Considering a more general situation of different backward rates ($\beta \neq w$) in the catalytic pathways will not change the qualitative picture of dynamic catalysis as we explicitly show in the Supporting Information (see Figures S3 and S4). From eq 14, one can determine the range of parameters at which the dynamic catalysts are more efficient, i.e., when EF > 1. It can be shown that this range of parameters is specified by the inequality

$$(x-1)[(u_0+u_1+w)(u_0x-u_1)+((u_0-u_1-w)x + (u_0-u_1+w))\gamma] < 0 \quad (15)$$

To understand better for what conditions dynamic catalysis is more efficient than static catalysis, it is convenient to consider two different situations depending on what step in the chemical reaction is slower.

Case 1 ($\mathbf{u_0} > \mathbf{u_1}$): this is the situation when the second step in the catalytic pathway along the site A is slower than the first step. It is schematically shown in Figure 2a,b. If $x > 1$, the second transition rate along the catalytic pathway B is even slower, and it is clear that transitions between these two pathways will not make dynamic catalysis more efficient than static catalysis. This is because the system will always face large kinetic barriers from the intermediate states (see Figure 2b), and jumping between pathways will not help. This argument is fully consistent with the analysis of expression eq 15, and it is also illustrated for specific calculations in Figure 3a. Thus, for $x > 1$, we always have EF < 1 independently of varying other kinetic parameters, and static catalysis is always a better option to accelerate the chemical reactions.

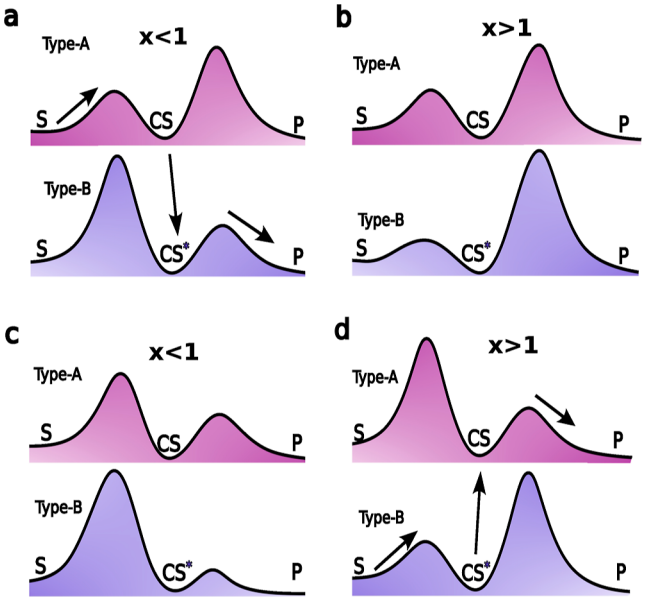

Figure 2. Schematic energy profiles for chemical reactions on the dynamic catalyst: (a) for $u_0 > u_1$ and $x < 1$ (case 1); (b) for $u_0 > u_1$ and $x > 1$ (case 1); (c) for $u_0 < u_1$ and $x > 1$ (case 2); and (d) for $u_0 < u_1$ and $x > 1$ (case 2). Dynamic catalysis is efficient only in the cases (a,d).

Then, the conditions for dynamic catalysis to be more efficient (EF > 1) might occur only for $x < 1$. This situation is illustrated in Figure 2a. Since the second transition is always slow in the catalytic pathway A, jumping to the catalytic pathway B with a low second barrier will make the overall process more efficient. The system is not trapped in the intermediate state and can create product molecules faster. This is also confirmed by the results presented in Figure 3a. However, dynamic catalysis is not always efficient even for $x < 1$, and this depends on the speed of fluctuations between catalytic pathways γ. For very large γ, the system can always escape traps in front of the slow transitions with large barriers (second step in pathway A and first step in pathway B): see blue and green curves in Figure 3a. However, there is a critical value of the fluctuation rate

$$\gamma_{c1} = \frac{u_1(u_0+u_1+w)}{u_0-u_1+w} \quad (16)$$

such that for $\gamma < \gamma_{c1}$, there is only a range of parameters, $x_c < x < 1$, at which the dynamic catalysts are more efficient (see the red curve in Figure 3a), with

$$x_c = \frac{u_1(u_0+u_1+w)-\gamma(u_0-u_1+w)}{u_0(u_0+u_1+w)-\gamma(u_1-u_0+w)} \quad (17)$$

This observation can be explained using the following arguments. Decreasing the parameter x from $x = 1$ increases the first barrier (rate α_0) and decreases the second barrier (rate α_1) in pathway B. For the given fluctuation rate γ, the increase in the first barrier is becoming so large that the system is not able to escape this trap fast enough, and the static catalysts are faster in this case (Figure 3a).

Our theoretical analysis also allows us to understand the role of fluctuations between different catalytic pathways, which is illustrated in Figure 3b. As expected, for the given set of parameters, increasing the rate γ always moves the system in the direction of making dynamic catalysts more efficient. While it eventually happens for $x < 1$ (red and green curves in Figure 3b), it will never happen for $x > 1$ (blue curve in Figure 3b), as we already explained above.

Case 2 ($\mathbf{u_0} < \mathbf{u_1}$): this is the situation when the first step in the catalytic pathway A is slower than the second step, as schematically shown in Figures 2c,d. Then, for $x < 1$, the first step in the catalytic pathway B will be even slower than for pathway A. So, we will have a system with two large barriers for the substrate associations, and jumping between the pathways will not help (Figure 2c). Clearly, for $x < 1$, static catalysis is always more efficient, as also illustrated by the results presented in Figure 3c. At the same time, the dynamic catalysts might be more efficient for $x > 1$, which is shown in Figure 2d, but not for all ranges of parameters. Again, there is a critical value of the fluctuation rate γ_{c2} that separates two different regimes

$$\gamma_{c2} = \frac{u_0(u_0+u_1+w)}{u_1-u_0+w} \quad (18)$$

For fast transitions between catalytic pathways A and B ($\gamma > \gamma_{c2}$), the system is always able to escape traps before large barriers, and dynamic catalysis is the most efficient method (EF > 1); see blue and green curves in Figure 3c. However, for smaller fluctuation rates ($\gamma < \gamma_{c2}$), the escape from the traps works only for $1 < x < x_c$ where the critical parameter x_c is given in eq 17. This is shown in Figure 3c (red curve). For large values of x beyond this critical value, the escape from the traps before large barriers is not possible. Again, for the fixed

https://doi.org/10.1021/acs.jpcc.4c02713
J. Phys. Chem. C 2024, 128, 9077−9089

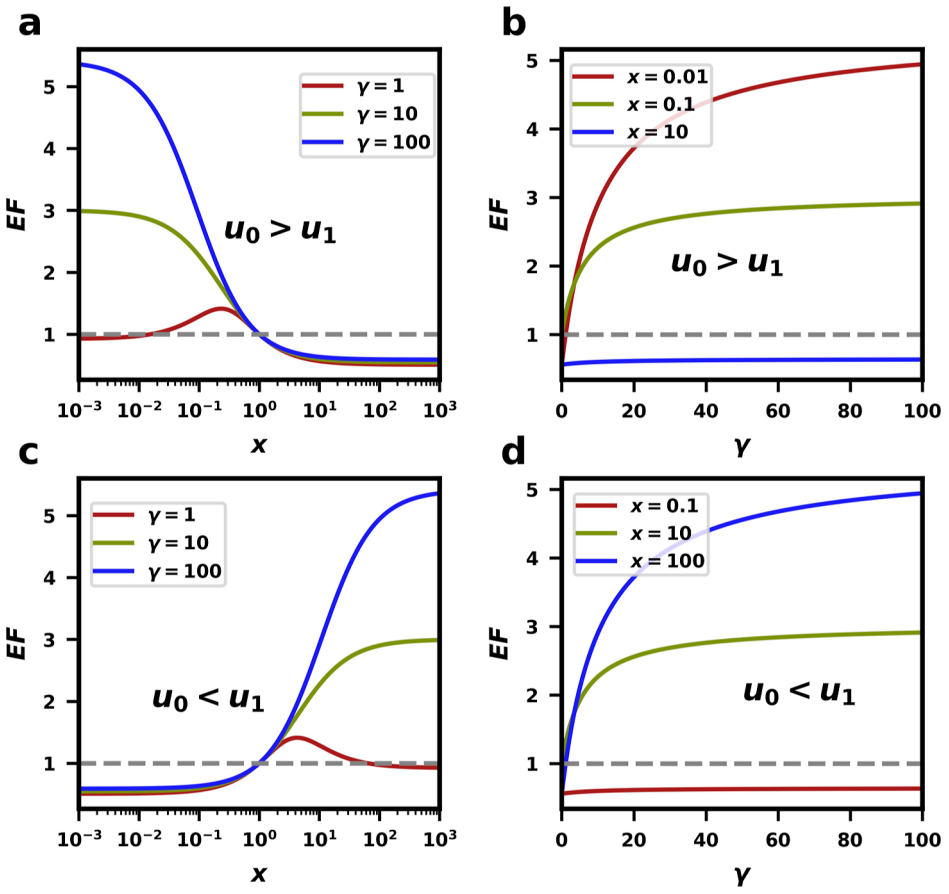

Figure 3. Temporal efficiency of dynamics catalysis. (a) Efficiency parameter EF as a function of x for different fluctuation rates γ for case 1. (b) Efficiency parameter EF as a function of the fluctuation rate γ for different x for case 1. The following parameters have been utilized in calculations: $u_0 = 10\ s^{-1}$ and $u_1 = w = 1\ s^{-1}$. (c) Efficiency parameter EF as a function of x for different fluctuation rates γ for case 2. (d) Efficiency parameter EF as a function of the fluctuation rate γ for different x for case 2. The following parameters have been utilized in calculations: $u_1 = 10\ s^{-1}$ and $u_0 = w = 1\ s^{-1}$.

set of kinetic rates, increasing the fluctuation rate γ always increases the efficiency of the system, but only for some range of parameters. It is still not enough to make dynamic catalysis always faster than static catalysis for these parameters (Figure 3d). In addition, we estimated the efficiency of dynamic catalysis for more general situations where the transition rates between different catalytic pathways are not equal, and similar trends are observed for these situations; see the Supporting Information (Figure S7) for more details.

Energy Dissipation in Dynamic Catalysis. Our theoretical analysis suggests that dynamic catalysts function better than static catalysts when the system can escape from the states that are facing large kinetic barriers. It is more convenient to think about it using the effective kinetic scheme for the processes, as shown in Figure 4a. Starting from the state 0 and considering for convenience the case 1 ($u_0 > u_1$ and $x < 1$), one can see that the system will quickly move to state 1 and state 2, but the product formation is very slow from these states. However, moving from the upper states to the lower states in Figure 4a allows the system to quickly create the product molecules because $\alpha_1 = u_1/x$. This suggests that paths $0 \rightarrow 1 \rightarrow 1^* \rightarrow 0^*$ and $0 \rightarrow 1 \rightarrow 2 \rightarrow 2^* \rightarrow 1^* \rightarrow 0^*$ are dominating when the system effectively catalyzes the chemical reactions. These processes generate circular fluxes in the effective kinetic scheme that one might associate with energy dissipation (entropy production).[39]

The notion of entropy production originates from stochastic thermodynamics and has been applied to small-scale systems like colloid particles, polymers, and molecular machines.[40−42] In these systems, external driving forces lead to a nonequilibrium steady state (NESS). Given our focus on a single-nanoparticle catalyst, the principles of stochastic thermodynamics can be conveniently extended to our system. At the microscopic level, the impact of fluctuations becomes significant, and the concept of entropy production provides a quantitative tool for distinguishing between systems with different degrees of deviations from equilibrium. The average rate of entropy production can be correlated with the energy or information exchange rate between the system and the heat bath.[41] Understanding the rate of energy dissipation is particularly relevant as it reflects the cost associated with sustaining specific dynamics within the system. Our theoretical approach can provide a quantitative assessment of how much energy can be dissipated and how it determines the efficiency of dynamic catalysis.

Generally, to evaluate energy dissipation in the nonequilibrium stationary state, one needs to know the fluxes and the affinities in the system.[39,43] More specifically, steady-state flux between two states i and j is given by

$$J_{ij} = r_{ij}P_i - r_{ji}P_j \tag{19}$$

https://doi.org/10.1021/acs.jpcc.4c02713
J. Phys. Chem. C 2024, 128, 9077−9089

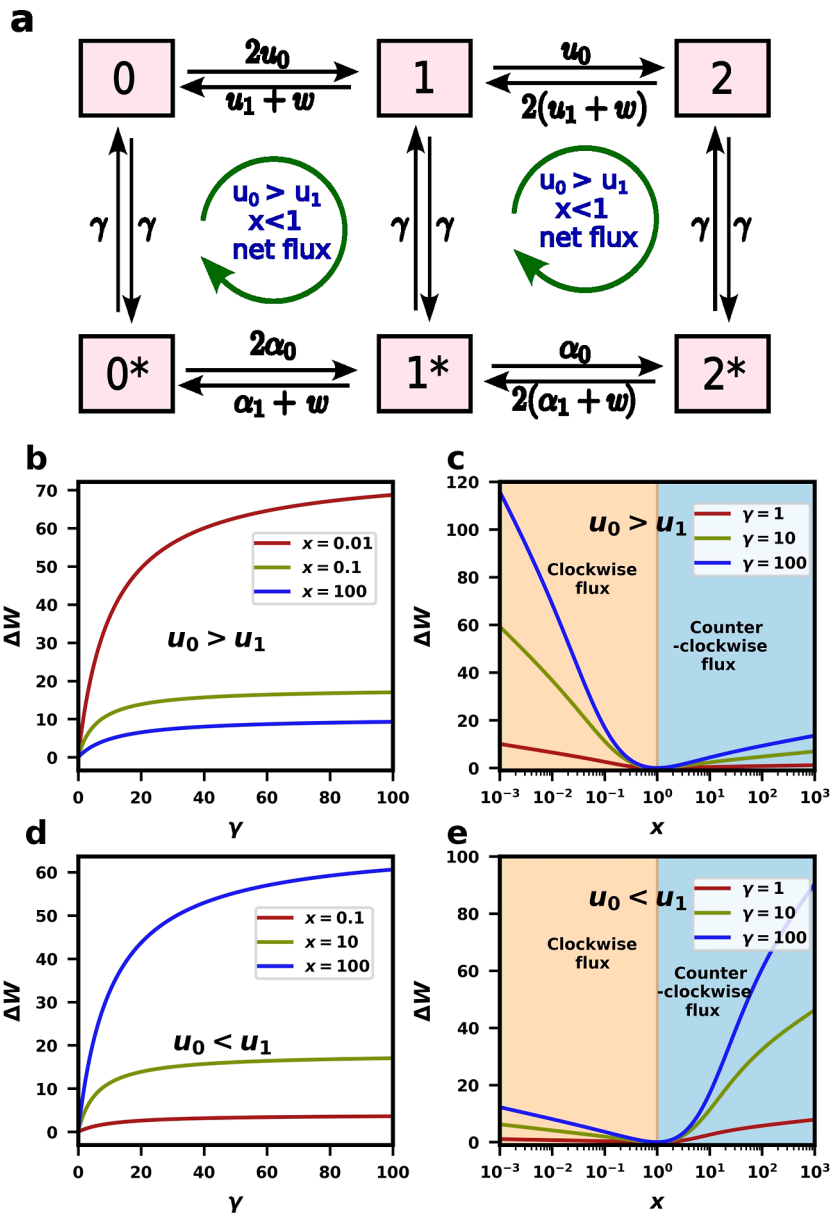

Figure 4. (a) Effective kinetic scheme for a system with alternation between two types of catalytic sites. (b) Energy dissipation parameter ΔW as a function of γ and (c) energy dissipation parameter ΔW as a function of x. The following kinetic rates used in calculations: $u_0 = 10\ s^{-1}$ and $u_1 = w = 1\ s^{-1}$. (d) Energy dissipation ΔW as a function of γ and (e) energy dissipation parameter ΔW as a function of x. The following kinetic rates used in calculations: $u_1 = 10\ s^{-1}$ and $u_0 = w = 1\ s^{-1}$.

where r_{ij} and r_{ji} are rates for transitions $i \to j$ and $j \to i$, respectively. P_i and P_j are stationary probabilities to find the system in state i or j. The affinity for the transitions $i \leftrightarrow j$ can be defined as (in units of k_BT)

$$A_{ij} = \ln\left(\frac{r_{ij}P_i}{r_{ji}P_j}\right) \tag{20}$$

One can think about this quantity as an effective free energy difference between the states j and i. Then, the energy dissipation (or entropy production) in the nonequilibrium system can be estimated as[43,44]

$$\Delta W = \frac{1}{2}\sum_{i,j} J_{i,j}A_{i,j} \tag{21}$$

The entropy production (energy dissipation) calculations are done by considering chemical reactions at all active sites, and this is accomplished by mapping the system into an effective kinetic model, which is a coarse-grained representation of the catalyst. In this theoretical framework, all the transitions are reversible, thereby enabling us to calculate affinities and to avoid singularities in the evaluation of energies. The transitions $n \to (n-1)$, $n^* \to (n^*-1)$ do not differentiate between the product formation and the substrate dissociation processes. As a result, the entropy production observed in our analysis includes contributions from both complex dissociation and product formation. However, we are only interested in the differences in energy dissipation between dynamic and static catalysis. Since both catalytic methods are treated at the same theoretical level, the results should help us

https://doi.org/10.1021/acs.jpcc.4c02713
J. Phys. Chem. C 2024, 128, 9077−9089

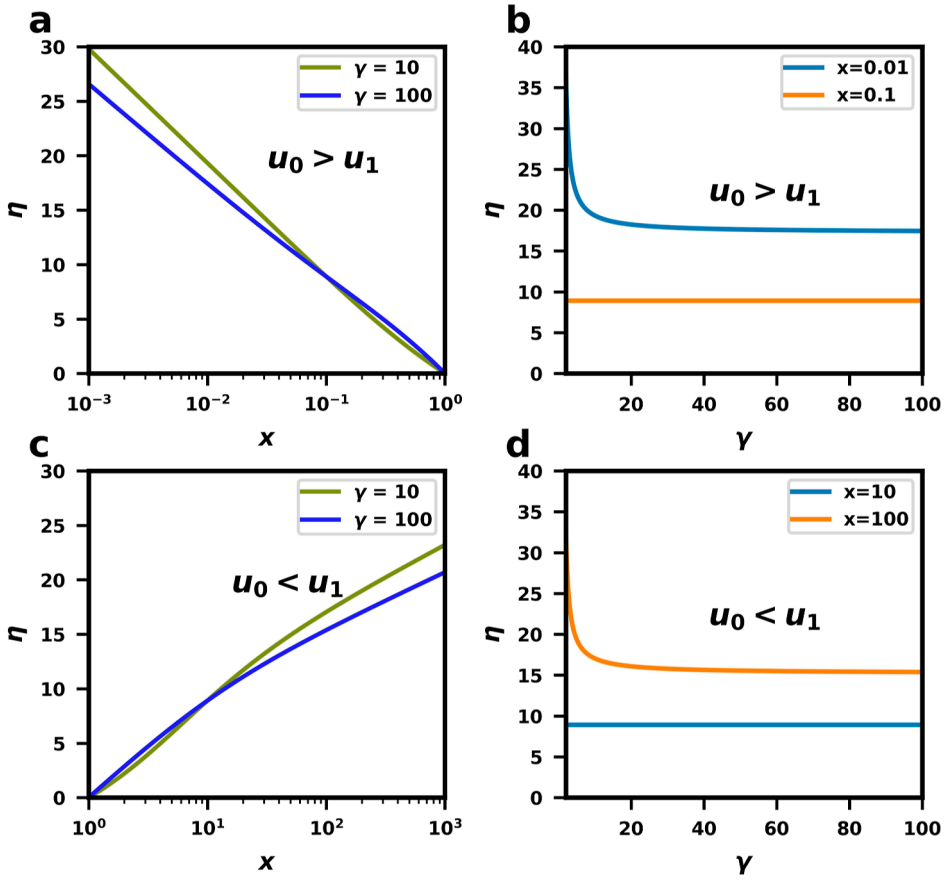

Figure 5. (a) Energy efficiency parameter η as a function of x and (b) as a function of the fluctuation speed γ with kinetic rates $u_0 = 10\ s^{-1}$ and $u_1 = w = 1\ s^{-1}$, corresponding to case 1. (c) Energy efficiency parameter η as a function of x and (d) as a function of the fluctuation speed γ with kinetic rates $u_1 = 10\ s^{-1}$ and $u_0 = w = 1\ s^{-1}$, corresponding to case 2.

to understand better the microscopic picture of dynamic catalysis.

Our stochastic model of dynamic catalysis (Figure 4a) allows us to explicitly evaluate all transition rates and all stationary probabilities. This provides a direct way of estimating the energy dissipation in dynamic catalysis. The detailed calculations are presented in the Supporting Information, yielding

$$\Delta W = \left\{ u_0\gamma(1-x)[u_1 + (u_1+w)x]\log\left(\frac{u_1 + wx}{(u_1+w)x^2}\right)\right\} / \{(u_0+u_1+w+\gamma)u_1 + [(u_0+u_1+w)w + (u_0+u_1+2w)\gamma]x + u_0(u_0+u_1+w+\gamma)x^2\} \quad (22)$$

where we again assumed that $\beta = w$. One can see that for $x = 1$ (static catalysis), there is no energy dissipation ($\Delta W = 0$), but all cases of dynamic catalysis ($x \neq 1$) are associated with energy dissipation; see also Figures 4c,e. Thus, dynamic catalysts always operate at nonequilibrium conditions. One can also conclude that to become more efficient, dynamic catalysis requires energy dissipation from fluctuations between macrostates, in contrast to static catalysis. At $x = 1$, both catalytic pathways A and B undergo the same chemical reactions. Under these conditions, the catalyst follows a detailed balance, resulting in zero energy dissipation from the point of view of an effective kinetic model. In this model, all clockwise and counterclockwise fluxes balance out each other. Since both macrostates are identical at $x = 1$ and no energy dissipation occurs, the dynamic behavior is absent. At the same time, it is important to emphasize that in real systems, there will be some additional energy dissipation even in the static catalysis case, and this means that our analysis estimates the relative energy dissipation in the dynamic catalysis in comparison with the static catalysis. Our result $\Delta W > 0$ simply means that more energy dissipation is needed for dynamic catalysts, and this catalytic mode is further from equilibrium than static catalysis.

Now, it is important to clarify how energy dissipation correlates with the efficiency of dynamic catalysis. Let us start with the range of parameters that correspond to case 1 ($u_0 > u_1$), as illustrated in Figures 4b,c. Increasing the fluctuation rate γ always leads to higher energy dissipation, but the effect is stronger for $x < 1$ when dynamic catalysis might be more efficient. Similarly, for case 2 ($u_0 < u_1$), faster alternation is associated with an increase in energy dissipation in the system. Again, when dynamic catalysis might be more efficient ($x > 1$), stronger energy dissipation is expected.

The results presented in Figure 4 show that to achieve a better performance for dynamic catalysis, the system has to spend some energy. Our theoretical approach can quantify this effect. For this purpose, we introduce an energy efficiency parameter

$$\eta = \frac{\Delta W}{\Delta \mathrm{EF}} \quad (23)$$

https://doi.org/10.1021/acs.jpcc.4c02713
J. Phys. Chem. C 2024, 128, 9077−9089

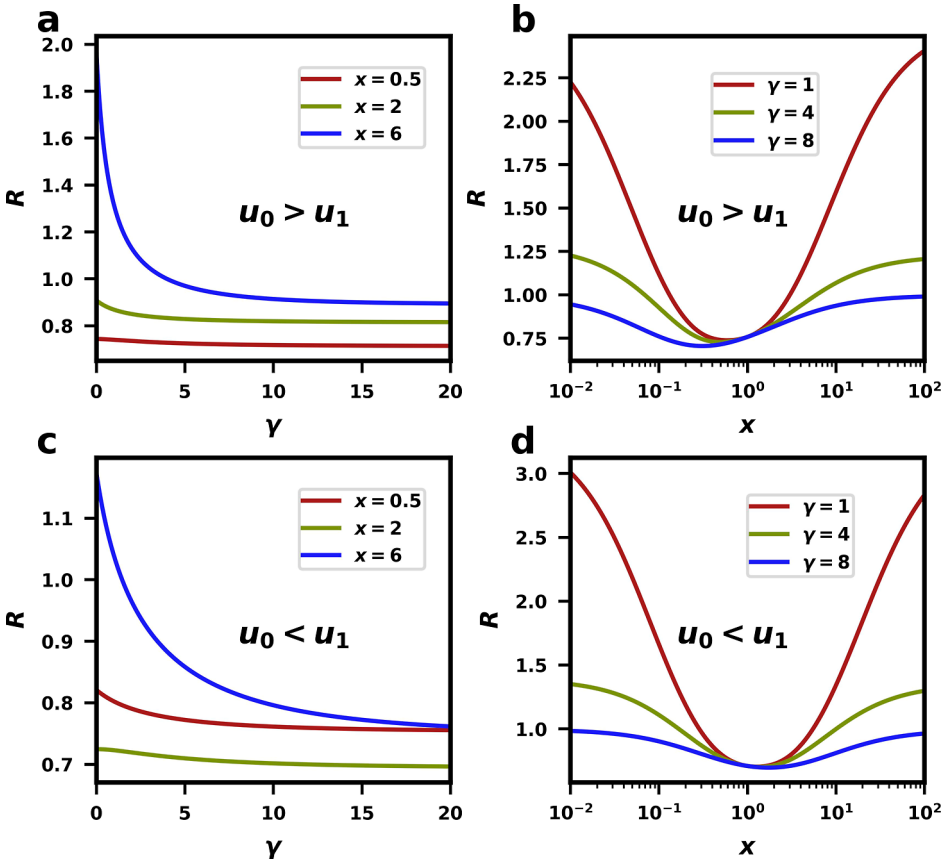

Figure 6. (a) Randomness as a function of the fluctuation speed γ and (b) randomness as a function of the parameter x. The following kinetic rates are used in calculations in plots (a,b): $u_0 = 8\ s^{-1}$, $u_1 = 3\ s^{-1}$, and $w = 2\ s^{-1}$, which corresponds to case 1. (c) Randomness as a function of the fluctuation speed γ and (d) randomness as a function of parameter x. The following kinetic rates are used in calculations for plots (c,d): $u_0 = 5\ s^{-1}$, $u_1 = 8\ s^{-1}$, and $w = 2\ s^{-1}$, which corresponds to case 2.

where $\Delta EF = EF - 1$. The physical meaning of this parameter is how much energy dissipation is needed to make dynamic catalysis more efficient than static catalysis. We expect that the most efficient catalytic system is achieved for the smallest values of this parameter since it would correspond to the smallest amount of energy needed to make catalysis more efficient.

Calculations are performed only for situations when the dynamic catalysts are more efficient ($EF > 1$), and the results are presented in Figure 5. One can see that lowering x (case 1) requires more energy dissipation (Figure 5a) to make dynamic catalysis more efficient. However, increasing the speed of fluctuation does not improve much the energy efficiency of dynamic catalysts; see Figure 5b. Increasing γ lowers the energy efficiency parameter but only for relatively small fluctuation rates and when $x \ll 1$. No improvement is observed for the values of x close to unity. Similar results are observed for case 2. Making dynamic catalysts more efficient by increasing x requires more energy dissipation (Figure 5c), but increasing the fluctuation speed again has a very limited effect (Figure 5d).

There is an important conclusion from the results presented in Figure 5. They suggest that a possible route to improve the efficiency of dynamic catalysis by accelerating the fluctuations between different catalytic pathways might be reasonable, but it is generally not the best strategy for a large range of parameters from the energetic point of view. It seems that increasing the energy dissipation (ΔW) becomes proportional to improvements in the catalytic efficiency (ΔEF) for large fluctuation rates γ.

Stochasticity of Dynamic Catalysis. Our focus on small systems emphasizes the significance of stochastic fluctuations in observable quantities. Numerous instances underscore the importance of stochastic effects, including biological systems like living cells,[45,46] physical phenomena such as phase transitions,[47] chemical kinetics, and nanocatalysts.[9] Our theoretical approach also allows us to estimate the degree of stochasticity in dynamic catalysis. For this purpose, we introduce a dimensionless parameter randomness (R), which is defined as[13,38,48]

$$R = \frac{\langle \tau^2 \rangle - \langle \tau \rangle^2}{\langle \tau \rangle^2} \tag{24}$$

The physical meaning of this parameter is the following. If the catalyzed chemical reaction of making a product from the substrate would be a single-step Poisson process, then it can be shown that $R = 1$.[48] However, deviations from unity reflect different sources of stochasticity in the system. The case $R < 1$ corresponds to the situation when there are several rate-limiting steps on the pathway between the initial and final states of the system. At the same time, $R > 1$ suggests the existence of multiple parallel pathways that might drive the system in opposite directions.

The results of our calculations of the randomness parameter R are presented in Figure 6. One can see that increasing the fluctuation rate γ generally decreases the randomness; see

https://doi.org/10.1021/acs.jpcc.4c02713
J. Phys. Chem. C 2024, 128, 9077−9089

Figures 6a,c. This can be understood in the following way. For not very fast fluctuations and for very large deviations from $x = 1$, the system might explore both catalytic pathways and $R > 1$ is observed. Increasing the rate γ changes the system from two-pathway dynamics to effectively single-pathway dynamics due to reaching the local equilibrium for alternation between macrostates A and B, as we argued before. In this case, R becomes smaller than 1. However, for x close to 1, the differences between the pathways are already not large, and we have $R < 1$ with not much effect on the randomness by varying the fluctuation rate γ.

The dependence of randomness on the parameter x is more complex, and it exhibits a nonmonotonic behavior with the minimal value of R at some x_{min}; see Figures 6b,d. Interestingly, x_{min} is not equal to one as one would naively expect; it is smaller than one for case 1 (Figure 6b) and larger than 1 for case 2 (Figure 6d). Again, this result might be explained by noticing that for x close to 1, both catalytic pathways are very similar, yielding small values of R, while for very large and small x, the differences between two pathways become large, increasing the randomness. In addition, faster alternation between different catalytic pathways makes this effect weaker.

One could also see (Figures 6b,d) that the position of x_{min} depends on the fluctuation rate. Increasing γ always shifts x_{min} away from 1. We can present the following arguments to explain these observations. When γ is small, transitions between macrostates A and B are less frequent, and the product molecules are typically formed only in one specific macrostate. Then, minimal randomness is expected when both rates in the same pathway are rate-limiting and comparable, i.e., for $\alpha_0 \simeq \alpha_1$. Using 10 this leads to the following estimate of x_{min}

$$x_{min} \simeq \sqrt{\frac{u_1}{u_0}} \tag{25}$$

The situation is different for very fast fluctuation rates ($\gamma \gg 1$). In this case, the process can be viewed as following a single pathway with the effective rate of substrate binding $(u_0 + \alpha_0)/2$ and the effective rate of product formation $(u_1 + \alpha_1)/2$. The minimum in randomness is expected when both of these rates are rate-limiting, yielding with the help of eq 10

$$x_{min} \simeq \frac{u_1}{u_0} \tag{26}$$

One should also notice that eqs 25 and 26 also explain why for case 1 we have $x_{min} < 1$ and for case 2 $x_{min} > 1$.

SUMMARY AND CONCLUSIONS

We developed a novel theoretical framework to understand the molecular mechanisms of dynamic catalysis that has been recently proposed as a new method of enhancing catalytic performance that avoids the limitations of static catalysis. Our method is based on the stochastic description that allows us to obtain a comprehensive quantitative description of these phenomena. In the presented theoretical method, chemical reactions at all active sites are simultaneously analyzed by mapping exactly dynamic processes into an effective kinetic model, providing a clearer microscopic picture of dynamic catalysis. In contrast to previous studies where external perturbations alter transition rates deterministically by changing the energy of the individual species (pumped/resonant catalysis), our study introduces stochastic fluctuations for the surfaces of the catalysts. Such surface transitions, driven by thermal energy, have been previously reported in some metal catalytic nanoclusters, causing the cage structure of the cluster to isomerize at higher temperatures and leading to various free-energy local minima states. Due to the thermal accessibility of these states, considering stochastic transitions between them seems to be a more realistic and more general approach. Figure S6 in the Supporting Information shows the comparative study of our model and pumped catalysts with deterministic oscillatory transitions, and one can see that the presented stochastic approach also accounts for all observations for deterministic transitions.

Our results show that the temporal efficiency of dynamic catalysis is determined only by the rates of chemical reactions and transitions between different pathways, but it is independent of the number of active sites. By explicitly analyzing a minimal theoretical model, it is found that alternating between different catalytic pathways might improve the catalytic performance; however, this happens only for some ranges of parameters. More specifically, large kinetic barriers must occur not for the same transitions in catalytic pathways, and the fluctuation rates must be fast enough to release the system from being trapped before large kinetic barriers in their pathways. Using an effective chemical-kinetic description, it is also shown that dynamic catalysis is a nonequilibrium phenomenon, and energy dissipation is required to make it more efficient than static catalysis. In addition, we analyzed the stochastic effects of dynamic catalysts that exhibit complex behavior depending on different parameters of the system. Furthermore, the temporal and energetic efficiency of dynamic catalysts is explicitly evaluated.

One of the main conclusions of this investigation is that, in contrast to previous studies, it is shown that dynamic catalysis does not always lead to improvements in the catalytic performance. In our theoretical analysis, we were able to quantitatively evaluate the conditions when it might happen, allowing us to present physical−chemical explanations of these observations. This result not only provided better microscopic picture of dynamic catalysis but also suggested practical ways to develop more efficient catalytic systems.

Although our theoretical approach provides a quantitative molecular picture of dynamic catalysis phenomena, it is important to discuss its limitations. Only two active sites ($N = 2$) on each catalytic surface have been assumed in our model, while in reality, the number of active sites might be very large ($N \gg 1$). It is clear how to generalize our method for the arbitrary number of active sites, but the calculations might become too complex to obtain explicit analytical results, and computer simulations seem to be a reasonable approach in this case. Note, however, that our calculations of temporal efficiency are already valid for an arbitrary number of active sites.

In this study, we explored dynamic catalysis phenomena where the active sites might transition between two catalytic pathways, following simple Michaelis−Menten or Langmuir−Hinshelwood like mechanisms with a single reversible intermediate step followed by irreversible product formation. How dynamic catalysis will perform for more complex catalytic mechanisms remains not well understood, as dealing with them poses analytical challenges. To prove that our simple model provides a generally valid physical−chemical description of these complex phenomena, one might consider catalytic reactions with multiple intermediate steps, as discussed in

https://doi.org/10.1021/acs.jpcc.4c02713
J. Phys. Chem. C 2024, 128, 9077−9089

the Supporting Information. Our Monte Carlo computational simulations for these more complex chemical mechanisms suggest that the qualitative results are consistent with one-step processes, justifying our theoretical analysis. Furthermore, the stochastic transitions are considered only between two catalytic pathways. This is inspired by the studies of thermal isomerization in metal nanoclusters, which might lead to distinct active sites. Nonetheless, it cannot be ruled out that the active sites might undergo partial transitions, creating several distinct heterogeneous catalytic pathways (with mixed active sites), and the system might fluctuate between them. This might lead to some new interesting phenomena that need to be further investigated. Our theoretical approach seems to be a good starting point for these future studies.

In addition, transitions between different catalytic macrostates might not be perfect as assumed in our work, and there might be multiple heterogeneous states with different fractions of different types of active sites. This can significantly complicate the analysis of dynamic catalysis. We also assumed a specific relation between kinetic rates for different pathways that generally might not hold. However, despite these issues, our theoretical approach still provides a transparent physical picture of dynamic catalysis that explains many important microscopic aspects of these phenomena and gives experimentally testable predictions. At the same time, more advanced experimental and theoretical studies of dynamic catalysts are clearly needed.

■ ASSOCIATED CONTENT

Supporting Information

The Supporting Information is available free of charge at https://pubs.acs.org/doi/10.1021/acs.jpcc.4c02713.

Detailed calculations for first-passage probability densities, steady-state probabilities, energy dissipation, and additional discussion on the findings and validity of the proposed model (PDF)

■ AUTHOR INFORMATION

Corresponding Authors

Srabanti Chaudhury − *Department of Chemistry, Indian Institute of Science Education and Research, Pune, Maharashtra 411008, India;* orcid.org/0000-0001-6718-8886; Email: srabanti@iiserpune.ac.in

Anatoly Kolomeisky − *Department of Chemistry, Rice University, Houston, Texas 77005, United States; Center for Theoretical Biological Physics, Department of Chemical and Biomolecular Engineering, and Department of Physics and Astronomy, Rice University, Houston, Texas 77005, United States;* orcid.org/0000-0001-5677-6690; Email: tolya@rice.edu

Author

Pankaj Jangid − *Department of Chemistry, Indian Institute of Science Education and Research, Pune, Maharashtra 411008, India*

Complete contact information is available at: https://pubs.acs.org/10.1021/acs.jpcc.4c02713

Author Contributions

#S.C. and A.K. contributed equally.

Notes

The authors declare no competing financial interest.

■ ACKNOWLEDGMENTS

ABK acknowledges the support from the Welch Foundation (C-1559), the NSF (CHE-2246878), and the Center for Theoretical Biological Physics sponsored by the NSF (PHY-2019745). S.C. acknowledges support from SERB Power Fellowship (SPF/2022/000155). P.J. acknowledges IISER Pune for fellowship.

■ REFERENCES

(1) Ertl, G.; Knozinger, H.; Weitkamp, J. *Handbook of Heterogeneous Catalysis*; VCH: Weinheim, 1997.

(2) Ross, J. R. *Heterogeneous Catalysis: Fundamentals and Applications*; Elsevier, 2011.

(3) Somorjai, G. A.; Li, Y. *Introduction to Surface Chemistry and Catalysis*; John Wiley & Sons, 2010.

(4) Fechete, I.; Wang, Y.; Védrine, J. C. The past, present and future of heterogeneous catalysis. *Catal. Today* **2012**, *189*, 2−27.

(5) Wang, Q.; Astruc, D. State of the Art and Prospects in Metal-Organic Framework (MOF)-Based and MOF-Derived Nanocatalysis. *Chem. Rev.* **2020**, *120*, 1438−1511.

(6) Bavykina, A.; Kolobov, N.; Khan, I. S.; Bau, J. A.; Ramirez, A.; Gascon, J. Metal-Organic Frameworks in Heterogeneous Catalysis: Recent Progress, New Trends, and Future Perspectives. *Chem. Rev.* **2020**, *120*, 8468−8535.

(7) Verboekend, D.; Pérez-Ramírez, J. Design of hierarchical zeolite catalysts by desilication. *Catal. Sci. Technol.* **2011**, *1*, 879−890.

(8) Corma, A.; Garcia, H. Supported gold nanoparticles as catalysts for organic reactions. *Chem. Soc. Rev.* **2008**, *37*, 2096−2126.

(9) Xu, W.; Kong, J. S.; Yeh, Y.-T. E.; Chen, P. Single-molecule nanocatalysis reveals heterogeneous reaction pathways and catalytic dynamics. *Nat. Mater.* **2008**, *7*, 992−996.

(10) Chen, D.; Shang, C.; Liu, Z.-P. Machine-learning atomic simulation for heterogeneous catalysis. *npj Comput. Mater.* **2023**, *9*, 2.

(11) Schlexer Lamoureux, P.; Winther, K. T.; Garrido Torres, J. A.; Streibel, V.; Zhao, M.; Bajdich, M.; Abild-Pedersen, F.; Bligaard, T. Machine Learning for Computational Heterogeneous Catalysis. *ChemCatChem* **2019**, *11*, 3581−3601.

(12) Chaudhury, S.; Singh, D.; Kolomeisky, A. B. Theoretical Investigations of the Dynamics of Chemical Reactions on Nanocatalysts with Multiple Active Sites. *J. Phys. Chem. Lett.* **2020**, *11*, 2330−2335.

(13) Chaudhury, S.; Jangid, P.; Kolomeisky, A. B. Dynamics of chemical reactions on single nanocatalysts with heterogeneous active sites. *J. Chem. Phys.* **2023**, *158*, 074101.

(14) Sun, G.; Alexandrova, A. N.; Sautet, P. Pt8 cluster on alumina under a pressure of hydrogen: Support-dependent reconstruction from first-principles global optimization. *J. Chem. Phys.* **2019**, *151*, 194703.

(15) Vojvodic, A.; Nørskov, J. K. New design paradigm for heterogeneous catalysts. *Natl. Sci. Rev.* **2015**, *2*, 140−143.

(16) Sabatier, P. *La Catalyse en Chimie Organique*; C. Béranger, 1920.

(17) Medford, A. J.; Vojvodic, A.; Hummelshøj, J. S.; Voss, J.; Abild-Pedersen, F.; Studt, F.; Bligaard, T.; Nilsson, A.; Nørskov, J. K. From the Sabatier principle to a predictive theory of transition-metal heterogeneous catalysis. *J. Catal.* **2015**, *328*, 36−42.

(18) Wodrich, M. D.; Sawatlon, B.; Busch, M.; Corminboeuf, C. The Genesis of Molecular Volcano Plots. *Acc. Chem. Res.* **2021**, *54*, 1107−1117.

(19) Ardagh, M. A.; Birol, T.; Zhang, Q.; Abdelrahman, O. A.; Dauenhauer, P. J. Catalytic resonance theory: SuperVolcanoes, catalytic molecular pumps, and oscillatory steady state. *Catal. Sci. Technol.* **2019**, *9*, 5058−5076.

(20) Ardagh, M. A.; Abdelrahman, O. A.; Dauenhauer, P. Principles of Dynamic Heterogeneous Catalysis: Surface Resonance and Turnover Frequency Response. *ACS Catal.* **2019**, *9*, 6929−6937.

(21) Gathmann, S. R.; Ardagh, M. A.; Dauenhauer, P. J. Catalytic resonance theory: Negative dynamic surfaces for programmable catalysts. *Chem Catal.* **2022**, *2*, 140−163.
(22) Shetty, M.; Walton, A.; Gathmann, S. R.; Ardagh, A.; Gopeesingh, J.; Resasco, J.; Birol, T.; Zhang, Q.; Tsapatsis, M.; Vlachos, D. G.; et al. The Catalytic Mechanics of Dynamic Surfaces: Stimulating Methods for Promoting Catalytic Resonance. *ACS Catal.* **2020**, *10*, 12666−12695.
(23) Zhang, Z.; Du, V.; Lu, Z. Energy landscape design principle for optimal energy harnessing by catalytic molecular machines. *Phys. Rev. E* **2023**, *107*, L012102.
(24) Zhai, H.; Alexandrova, A. N. Fluxionality of Catalytic Clusters: When It Matters and How to Address It. *ACS Catal.* **2017**, *7*, 1905−1911.
(25) Sergeeva, A. P.; Popov, I. A.; Piazza, Z. A.; Li, W.-L.; Romanescu, C.; Wang, L.-S.; Boldyrev, A. I. Understanding boron through size-selected clusters: structure, chemical bonding, and fluxionality. *Accounts Chem. Res.* **2014**, *47*, 1349−1358.
(26) Joshi, K.; Krishnamurty, S. Au 26: A case of fluxionality/co-existence. *Phys. Chem. Chem. Phys.* **2018**, *20*, 8616−8623.
(27) Ghosh, T.; Arce-Ramos, J. M.; Li, W.-Q.; Yan, H.; Chee, S. W.; Genest, A.; Mirsaidov, U. Periodic structural changes in Pd nanoparticles during oscillatory CO oxidation reaction. *Nat. Commun.* **2022**, *13*, 6176.
(28) Vincent, J. L.; Crozier, P. A. Atomic level fluxional behavior and activity of CeO2-supported Pt catalysts for CO oxidation. *Nat. Commun.* **2021**, *12*, 5789.
(29) Vendelbo, S. B.; Elkjær, C. F.; Falsig, H.; Puspitasari, I.; Dona, P.; Mele, L.; Morana, B.; Nelissen, B. J.; van Rijn, R.; Creemer, J. F.; et al. Visualization of oscillatory behaviour of Pt nanoparticles catalysing CO oxidation. *Nat. Mater.* **2014**, *13*, 884−890.
(30) Alcorn, F. M.; Jain, P. K.; van der Veen, R. M. Time-resolved transmission electron microscopy for nanoscale chemical dynamics. *Nat. Rev. Chem* **2023**, *7*, 256−272.
(31) Lawrence, E. L.; Levin, B. D.; Boland, T.; Chang, S. L.; Crozier, P. A. Atomic Scale Characterization of Fluxional Cation Behavior on Nanoparticle Surfaces: Probing Oxygen Vacancy Creation/Annihilation at Surface Sites. *ACS Nano* **2021**, *15*, 2624−2634.
(32) Poths, P.; Alexandrova, A. N. Theoretical Perspective on Operando Spectroscopy of Fluxional Nanocatalysts. *J. Phys. Chem. Lett.* **2022**, *13*, 4321−4334.
(33) Zhang, Z.; Zandkarimi, B.; Alexandrova, A. N. Ensembles of Metastable States Govern Heterogeneous Catalysis on Dynamic Interfaces. *Acc. Chem. Res.* **2020**, *53*, 447−458.
(34) Zhai, H.; Alexandrova, A. N. Ensemble-Average Representation of Pt Clusters in Conditions of Catalysis Accessed through GPU Accelerated Deep Neural Network Fitting Global Optimization. *J. Chem. Theory Comput.* **2016**, *12*, 6213−6226.
(35) Halder, A.; Ha, M. A.; Zhai, H.; Yang, B.; Pellin, M. J.; Seifert, S.; Alexandrova, A. N.; Vajda, S. Oxidative Dehydrogenation of Cyclohexane by Cu vs Pd Clusters: Selectivity Control by Specific Cluster Dynamics. *ChemCatChem* **2020**, *12*, 1307−1315.
(36) Zhang, Z.; Cui, Z. H.; Jimenez-Izal, E.; Sautet, P.; Alexandrova, A. N. Hydrogen Evolution on Restructured B-Rich WB: Metastable Surface States and Isolated Active Sites. *ACS Catal.* **2020**, *10*, 13867−13877.
(37) Punia, B.; Chaudhury, S.; Kolomeisky, A. B. Understanding the Reaction Dynamics on Heterogeneous Catalysts Using a Simple Stochastic Approach. *J. Phys. Chem. Lett.* **2021**, *12*, 11802−11810.
(38) Singh, D.; Chaudhury, S. A stochastic theoretical approach to study the size-dependent catalytic activity of a metal nanoparticle at the single molecule level. *Phys. Chem. Chem. Phys.* **2017**, *19*, 8889−8895.
(39) Qian, H. Nonequilibrium steady-state circulation and heat dissipation functional. *Phys. Rev. E* **2001**, *64*, 022101.
(40) Rocha, B. C.; Paul, S.; Vashisth, H. Role of Entropy in Colloidal Self-Assembly. *Entropy* **2020**, *22*, 877.
(41) Seifert, U. Stochastic thermodynamics, fluctuation theorems and molecular machines. *Rep. Prog. Phys.* **2012**, *75*, 126001.
(42) Endres, R. G. Entropy production selects nonequilibrium states in multistable systems. *Sci. Rep.* **2017**, *7*, 14437.
(43) Qian, H.; Kjelstrup, S.; Kolomeisky, A. B.; Bedeaux, D. Entropy production in mesoscopic stochastic thermodynamics: nonequilibrium kinetic cycles driven by chemical potentials, temperatures, and mechanical forces. *J. Phys.: Condens. Matter* **2016**, *28*, 153004.
(44) Schnakenberg, J. Network theory of microscopic and macroscopic behavior of master equation systems. *Rev. Mod. Phys.* **1976**, *48*, 571−585.
(45) Shahrezaei, V.; Swain, P. S. The stochastic nature of biochemical networks. *Curr. Opin. Biotechnol.* **2008**, *19*, 369−374.
(46) Wilkinson, D. J. Stochastic modelling for quantitative description of heterogeneous biological systems. *Nat. Rev. Genet.* **2009**, *10*, 122−133.
(47) Henkel, M. *Non-Equilibrium Phase Transitions*; Springer, 2008.
(48) Kolomeisky, A. B. *Motor Proteins and Molecular Motors*; CRC Press, 2015.

https://doi.org/10.1021/acs.jpcc.4c02713
J. Phys. Chem. C 2024, 128, 9077−9089